Supporting Information

Lim et al. 10.1073/pnas.1316557110

SI Text

Lattice Parameters. Lattice parameters of the pristine, intermediate, and fully charged phases are as follows.

Pristine phase: a = 14.225 Å, b = 14.225 Å, c = 6.364 Å

Intermediate phase: a = 14.2457 Å, b = 14.2457 Å, c = 6.3684 Å

Fully-charged phase: a = 14.541 Å, b = 14.541 Å, c = 6.240 Å

The whole pattern fitting for the fully charged phase is presented in Fig. S4.

Integration of Reduced Graphene Oxide for Improved Cell Performance. In an attempt to achieve even better electrochemical performance, we integrated $Na_7V_4(P_2O_7)_4PO_4$ with reduced graphene oxide (rGO). The improved electrochemical performances based on the rGO integration have been reported in a wide range of battery electrode materials owing to the high electrical conductivity, good mechanical properties, and large surface area of rGO. The crystal structure and size of particles are not altered by rGO integration and the rGO layers with thicknesses of ∼10 nm cover $Na_7V_4(P_2O_7)_4PO_4$ particles (Fig. S2).

Electrochemical Properties of the Graphene-Integrated $Na_7V_4(P_2O_7)_4PO_4$. The galvanostatic profiles (Fig. S3*A*) of the rGO-integrated sample, namely rGO $Na_7V_4(P_2O_7)_4PO_4$, exhibit potential plateaus at 3.88 V consistent with the bare $Na_7V_4(P_2O_7)_4PO_4$ case. Moreover, the rGO integration increases the reversible capacity from 73.6 to 94.5 mAh·g^{-1} at C/20. The increased capacity of the integrated sample is ascribed to combined effects of nonfaradaic capacities from rGO surfaces and enhanced electric conductivity that activate a larger portion of $Na_7V_4(P_2O_7)_4PO_4$. All of the specific capacities addressed in this study are based on the mass of $Na_7V_4(P_2O_7)_4PO_4$ only because the exclusive contribution from rGO is difficult to isolate.

The enhanced electronic conductivity also endows rGO $Na_7V_4(P_2O_7)_4PO_4$ with excellent rate performance. As shown in Fig. S3*B*, even when the C rate increases 600 times from C/20–30C, 54.0% of the original capacity (96.5 mAh·g^{-1}) was retained. This rate performance is quite noticeable because a substantial capacity of 52.1 mAh·g^{-1} is available during 1-min discharging time even with micrometer particle dimensions. Also, ∼96.2% of the original capacities were recovered when the C rate returned to C/2 after high rate measurements at 10C and 30C, reconfirming the robust character of this material in electrochemical operations. The discharging potential profiles at various C rates are presented in Fig. S3*C*. In addition, the cycling performance of rGO $Na_7V_4(P_2O_7)_4PO_4$ at a lower rate of C/20 is displayed in Fig. S3*D*. rGO $Na_7V_4(P_2O_7)_4PO_4$ preserves 97.4% of the initial capacity (= 94.5 mAh·g^{-1}) after 50 cycles.

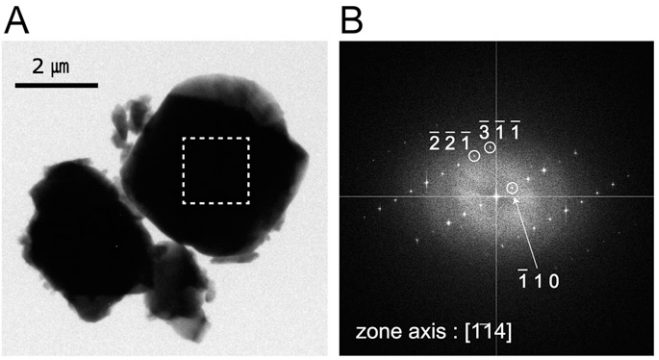

Fig. S1. (*A*) Transmission electron microscopy (TEM) image of the as-synthesized $Na_7V_4(P_2O_7)_4PO_4$. (*B*) A fast Fourier transformation pattern obtained from the white box in *A*.

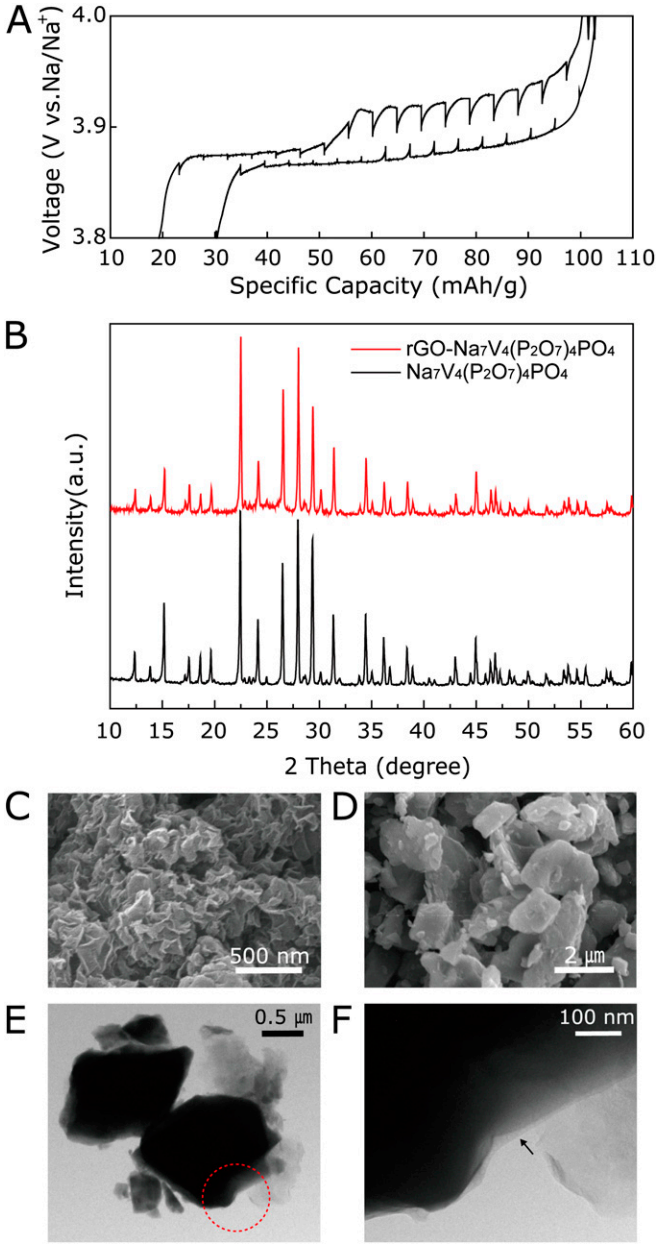

Fig. S2. (*A*) A QOCP profile of rGO $Na_7V_4(P_2O_7)_4PO_4$ measured at C/20. (*B*) X-ray diffraction (XRD) patterns of the pristine $Na_7V_4(P_2O_7)_4PO_4$ and rGO $Na_7V_4(P_2O_7)_4PO_4$. SEM images of (*C*) rGO and (*D*) rGO $Na_7V_4(P_2O_7)_4PO_4$. (*E*) A TEM image of rGO $Na_7V_4(P_2O_7)_4PO_4$ and (*F*) its magnified image from the red circle in *E*. The magnified image indicates that the rGO coating layer (arrow mark) is ~10 nm.

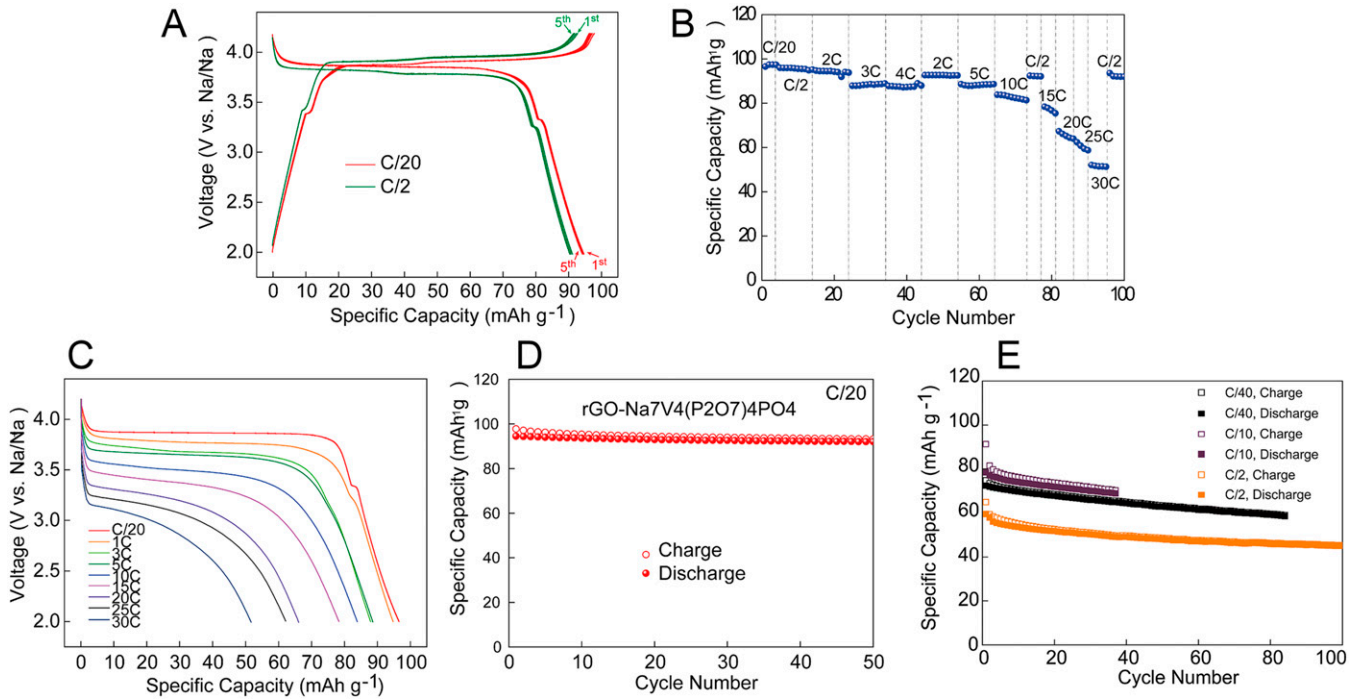

Fig. S3. (*A*) Galvanostatic profiles of rGO $Na_7V_4(P_2O_7)_4PO_4$ measured at C/2 and C/20. (*B*) The rate capability of rGO $Na_7V_4(P_2O_7)_4PO_4$. (*C*) Discharging voltage profiles of rGO $Na_7V_4(P_2O_7)_4PO_4$ at different C rates. (*D*) The capacity retentions of rGO $Na_7V_4(P_2O_7)_4PO_4$ for 50 cycles when measured at C/20. (*E*) Cycle lives of bare $Na_7V_4(P_2O_7)_4PO_4$ at various current rates.

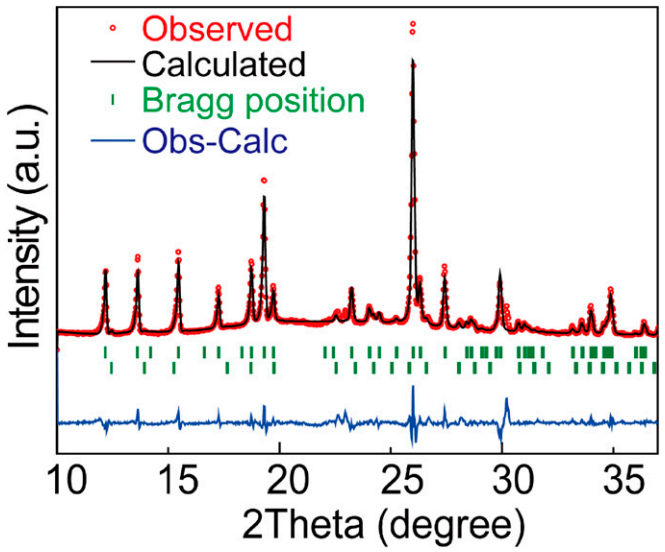

Fig. S4. The XRD spectrum and whole pattern fitting of $Na_7V_4(P_2O_7)_4PO_4$ after full charging [R_p = 5.42, R_{wp} = 7.98, χ^2 = 22.7, a (Å) = 14.541, b (Å) = 14.541, c (Å) = 6.240]. The upper and lower Bragg positions (green bars) correspond to those at the fully charged and pristine states. The pristine phase was also reflected in the whole pattern fitting of the fully charged state as a second phase.

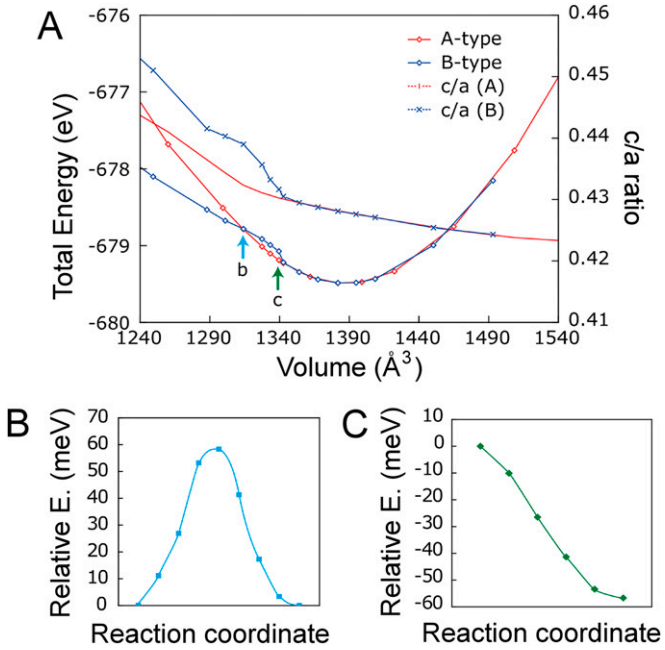

Fig. S5. (*A*) The energy curves as a function of volume for the fully charged composition, $Na_7V_4(P_2O_7)_4PO_4$, in the A-type and B-type structures. The phase transformation from the A type to the B type occurs through the rotation of the $(VP_2O_7)_4PO_4$ units accompanying the expansion of the cell volume. (*B* and *C*) The energy barriers of the phase transformation from the A-type to the B-type phases at the b and c points of *A*, respectively. The energy barrier is expected to be less than 60 meV for both A-to-B and B-to-A directions of the rotation.

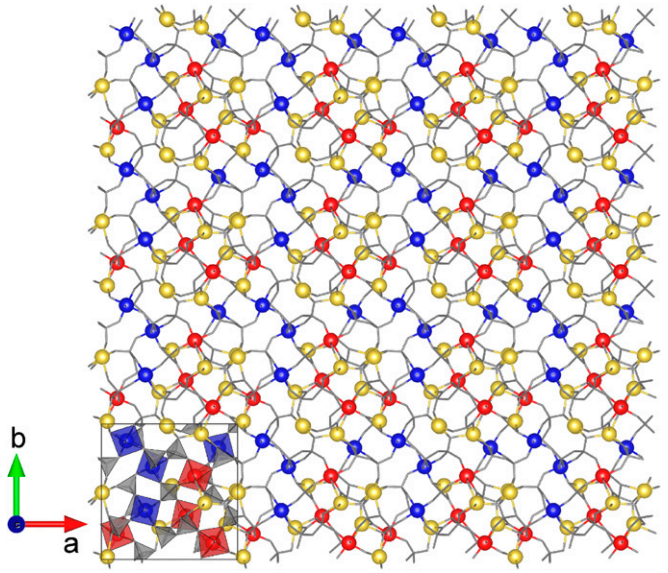

Fig. S6. The Na and V^{3+}/V^{4+} orderings of the intermediate phase, $Na_5V_4(P_2O_7)_4PO_4$, along the c-axis. Here, a-, b-, and c-axes are equivalent to x-, y-, and z-axes. The yellow, red, and blue spheres are Na^+, V^{3+}, and V^{4+} cations. Note that this is electrostatically the most stable ordering among all of the possible sodium and charge orderings at the given composition ($x = 5$).

Table S1. Detailed information for the Rietveld refinement of $Na_7V_4(P_2O_7)_4PO_4$ using the combined X-ray and neutron diffraction patterns

Crystal system	Tetragonal	
Space group	$P\text{-}42_1c$ (no. 114)	
a, Å	14.225 (3)	
b, Å	14.225 (3)	
c, Å	6.364 (17)	
Unit volume, Å	1,287.827	
Formula weight	1,155.439	
Source	X-ray	Neutron
Wavelength, Å	1.5418	1.834333
2θ range	10.10–110	0–159.95
No. of data points	4,996	3,200
No. of reflections	1,006	510
R_B, %	7.96	5.14
R_p, %	9.34	3.61
R_{wp}, %	12.9	4.64
R_{exp}, %	10.6	2.31
χ^2	1.49	4.02

No. 114 in the space group parentheses refers to corresponding crystallographic space group number, and the numbers in the parentheses in unit cell parameters indicate standard deviations.

Table S2. Atomic parameters for $Na_7V_4(P_2O_7)_4PO_4$ determined from the combined X-ray and neutron diffraction patterns

Atom	Site	*x/a*	*y/b*	*z/c*	B_{iso}, Å^2
V1	8e	0.1200 (4)	0.1834 (4)	0.1322 (9)	1.55 (13)
P1	8e	0.3037 (3)	0.0446 (4)	0.1108 (9)	1.41 (12)
P2	8e	0.2571 (4)	0.3803 (4)	0.1399 (7)	0.81 (11)
P3	2a	0	0	0	0.76 (2)
O1	8e	0.0550 (4)	0.0632 (4)	0.1481 (9)	1.15 (12)
O2	8e	0.3311 (4)	0.3632 (4)	0.3126 (8)	0.98 (13)
O3	8e	0.5022 (4)	0.2410 (4)	0.4187 (9)	1.74 (13)
O4	8e	0.0868 (4)	0.1966 (4)	0.4408 (8)	1.79 (15)
O5	8e	0.2443 (4)	0.1224 (4)	0.2055 (9)	0.86 (10)
O6	8e	0.1924 (4)	0.3004 (4)	0.1025 (9)	1.24 (12)
O7	8e	0.4030 (4)	0.0736 (4)	0.0685 (1)	1.63 (14)
O8	8e	0.1890 (3)	0.4646 (4)	0.2137 (8)	0.71 (12)
Na1	8e	0.5799 (5)	0.7606 (6)	0.0986 (13)	1.87 (18)
Na2	4d	0	0.5	0.170 (2)	1.87 (2)
Na3	2a	0.5	0.5	0	5.59 (6)

The numbers in the parentheses indicate standard deviations of atomic parameters.